Supporting Information

van der Velden et al. 10.1073/pnas.1010210108

SI Materials and Methods

Zebrafish Strains and Screening Methods. Zebrafish were maintained as previously described (1). An *N*-ethyl-*N*-nitrosourea (ENU) mutation library was used to screen mutations in zebrafish liver kinase B1 (lkb1). Sequence analysis identified two mutant alleles in exon 7; *lkb1*$^{Y245\times}$ and *lkb1* $^{Y260\times}$. F1 founder fish were out-crossed to AB and TL genetic backgrounds. In all experiments, *lkb1*$^{Y245\times/Y245\times}$, *lkb1*$^{Y260\times/Y260\times}$, and *lkb1*$^{Y245\times/Y260\times}$ were used with identical results. Genotype analysis for *lkb1*$^{Y245\times}$ and *lkb1*$^{Y260\times}$ was performed by PCR using the primer set *lkb1*_F: GATGCGATTTATCTTTGCAC, *lkb1*_R: GGAAGAGCAGAAAGGCTATG followed by sequence analysis for allele *lkb1*$^{Y245\times}$. Digestion of the PCR product with restriction enzyme Xba1 identified allele *lkb1*$^{Y260\times}$.

Histology, Immunohistochemistry, and Immunofluorescence. Larvae were fixed in 40% ethanol, 5% acetic acid, and 10% formalin (EAF) for 2 h at room temperature, followed by three washes in PBS with Triton-X (PBT) before being embedded in 1.5% low-melting agarose. Agarose pellets were dehydrated in ethanol, cleared in xylene, and processed into paraffin. Four-micrometer sections were stained with H&E.

For immunohistochemical staining, sections were deparaffinized and hydrated, followed by 15 min microwave antigen retrieval in 10 mM Tris, 1 mM EDTA, pH 9.0. Endogenous peroxidase activity was blocked in 3% H_2O_2 for 10 min. Sections were blocked in 5% goat serum (DakoCytomation) for 30 min at room temperature and incubated overnight at 4 °C in rabbit anti–phospho-AKT (Ser473) (1:50; #4060; Cell Signaling), rabbit anti–phospho-factor 4E binding protein 1 (4EBP1) (Thr-37/46) (1:50; #2855; Cell Signaling), and rabbit anti–phospho-S6 ribosomal protein (Ser240/244) (1:50; #2215; Cell Signaling). Secondary antibody was biotinylated goat anti-rabbit IgG (1:800; DakoCytomation). Sections were incubated with StreptABComplex/HRP (DakoCytomation) for 30 min followed by detection with 3,3′-diaminobenzidine (DAB) substrate-chromogen (DakoCytomation) and counterstaining with hematoxylin.

For immunofluorescence analysis, sections were deparaffinized and hydrated, followed by microwave antigen retrieval for 15 min in preheated 1.9 mM citric acid, 8.2 mM sodium citrate, pH 6.0, or in preheated 10 mM Tris, 1 mM EDTA, pH 9.0. Sections were blocked in PBS containing 5% normal goat serum for 30 min at room temperature and incubated in primary antibody overnight at 4 °C. Primary antibodies used were rabbit anti-PKC ζ (1:200; Santa Cruz), mouse anti–β-catenin (1:100; BD Biosciences), mouse anti–E-cadherin (1:100; BD Biosciences), rabbit anti–ZO-1 (1:200; Zymed Laboratories) and rabbit anti-sodium/potassium ATPase (1:100; Developmental Studies Hybridoma Bank). Secondary antibodies were anti-rabbit Alexa Fluor 568 and anti-mouse Alexa Fluor 568 (1:200; Molecular Probes). Nuclei were stained with DAPI.

Antibodies Used for Western Blot Analyses. Antibodies used for Western blot analyses were rabbit anti–acetyl-CoA carboxylase (1:500; #3662; Cell Signaling), rabbit anti–phospho-acetyl-CoA carboxylase (Ser79) (1:500; #3661; Cell Signaling), rabbit anti-AMPK (1:500; #2531; Cell Signaling), rabbit anti–phospho-AMPKα (Thr-172) (1:500; #2532; Cell Signaling), rabbit anti-p70 S6 kinase (1:500; #9202; Cell Signaling), mouse anti–phospho-p70 S6 kinase (Thr389) (1:500; #9206; Cell Signaling), mouse anti-ribosomal S6 protein (1:500; #2317; Cell Signaling), rabbit anti–phospho-S6 ribosomal protein (Ser240/244) (1:50; #2215; Cell Signaling), rabbit anti-4EBP1 (1:500; #9644; Cell Signaling), rabbit anti–phospho-S6 ribosomal protein (Ser240/244) (1:500; #221; Cell Signaling), mouse anti–β-actin (1:5,000; #ab6276; Abcam), and mouse anti-tubulin (1:5,000; #T9026; Sigma Aldrich). Secondary antibodies used were goat anti-mouse IgG (1:10.000; Zymed) and goat anti-rabbit IgG (1:10.000; BioSource). Proteins were detected using ECL (Amersham) followed by exposure to high-performance autoradiography films (Amersham).

Oil Red O. Larvae were fixed in 4% paraformaldehyde (PFA) overnight at 4 °C. After three washings in PBS, larvae were infiltrated with a graded series of propylene glycol. Staining with freshly filtered 0.5% Oil Red O in 100% propylene glycol was performed overnight at room temperature on an orbital shaker (GFL-3016). Whole-mount images were captured on a Leica CCD camera. Stained larvae were embedded in 4% low-melting agarose, and 50-μm sections were obtained by vibratome sectioning (Microm HM 650 V).

Periodic Acid-Schiff Staining. Larvae were fixed in 4% PFA overnight at 4 °C. After three washings in PBT, larvae were permeabilized in 40 μg/mL proteinase K for 30 min at room temperature. Specimens were washed three times in PBT, rinsed in milli-Q (MQ) water, and oxidized in periodic acid for 30 min at room temperature. After three 20-min washings, larvae were stained with Schiff reagent for 30 s followed by immediate rinsing in tap water. Stained larvae were sectioned by vibratome as described above.

Whole-Mount in Situ Hybridization. Whole-mount in situ hybridizations were carried out as described previously (1) with the following modifications: Larvae were permeabilized with 10 μg/mL proteinase K for 90 min at room temperature. Riboprobes for *lkb1* (MDR1734-97029820; Open Biosystems), insulin-like growth factor (IGF)-binding protein 1 (*igfbp1*) (amplified from genomic DNA; forward: cggaattcctgggtggcagcattcag; reverse: gctctagactgtctcgctttggctgtg), lactate dehydrogenase a (*ldha*) (2), and NADH dehydrogenase (ubiquinone) 1 α subcomplex 4 (*ndufa4*) (2) were synthesized by in vitro transcription. Hybridization was performed overnight at 68–70 °C with 500 ng anti-sense RNA probe per 500 μL. Larvae were developed in nitro blue tetrazolium/ 5-bromo-4-chloro-3-indolyl phosphate (NBT/BCIP) (Roche) by incubation at room temperature for a few hours or overnight at 4 °C.

Metabolic Rate Assay. The metabolic rate assay was performed essentially as described in ref. 3 with the following modifications: Larvae were raised in assay medium that consists of reverse osmosis-purified water with added mineral salts (Sera mineral salts) to obtain a conductivity of 350 μS/cm. Larvae were rinsed three times with pH 8.5-adjusted assay medium to which 0.01% wt/vol phenol red was added. Larvae then were transferred manually into wells of a 96-well flat-bottomed plate (Fluka) in 50 μL assay medium. Wells were covered with 100 μL mineral oil to limit gas exchange, and absorbance of phenol red at 570 nm was measured on a microplate reader (Tecan Infinite M200) for 1 h. A modified Henderson–Hasselbalch equation, $A_{570} = [K^* (A_{570(max)})/(H^+ + K)] + A_{570(min)}$, was used to convert absorbance to moles of acid. $A_{570(min)}$ and $A_{570(max)}$ were determined using an empiric titration curve. $A_{570(min)} = 0.05$; $A_{570(max)} = 0.90$; calculated parameter $K = 1.20.10^{-08}$.

ATP Measurements. Total ATP was measured with the ENLITEN luciferase ATP assay kit (Promega) following the manufacturer's instructions. Individual embryos (eight per genotype) were homogenized in 1% trichloroacetic acid (TCA), the lysate was diluted 200 times in acetate buffer (pH 7.75), and luminescence was measured in a Berthold luminometer. The amount of light produced is proportional to the amount of ATP in the sample. Measurements are given in relative light units (RLU).

1. Westerfield M (2000) *The Zebrafish Book* (Univ of Oregon Press, Eugene, OR), 4th Ed.
2. van Rooijen E, et al. (2009) Zebrafish mutants in the von Hippel-Lindau tumor suppressor display a hypoxic response and recapitulate key aspects of Chuvash polycythemia. *Blood* 113:6449–6460.
3. Makky K, Duvnjak P, Pramanik K, Ramchandran R, Mayer AN (2008) A whole-animal microplate assay for metabolic rate using zebrafish. *J Biomol Screen* 13:960–967.

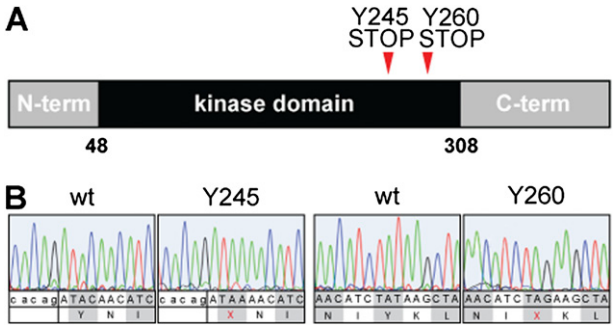

Fig. S1. (*A*) Schematic representation of the zebrafish Lkb1 protein depicting the location of the two recovered *lkb1* mutations. [In the Y245 allele a C-to-A substitution leads to a premature stop codon (TAA). In the Y260 allele, a T-to-G substitution leads to a premature stop codon (TGA)]. (*B*) Sequence peaks at the sites of the *lkb1* mutations.

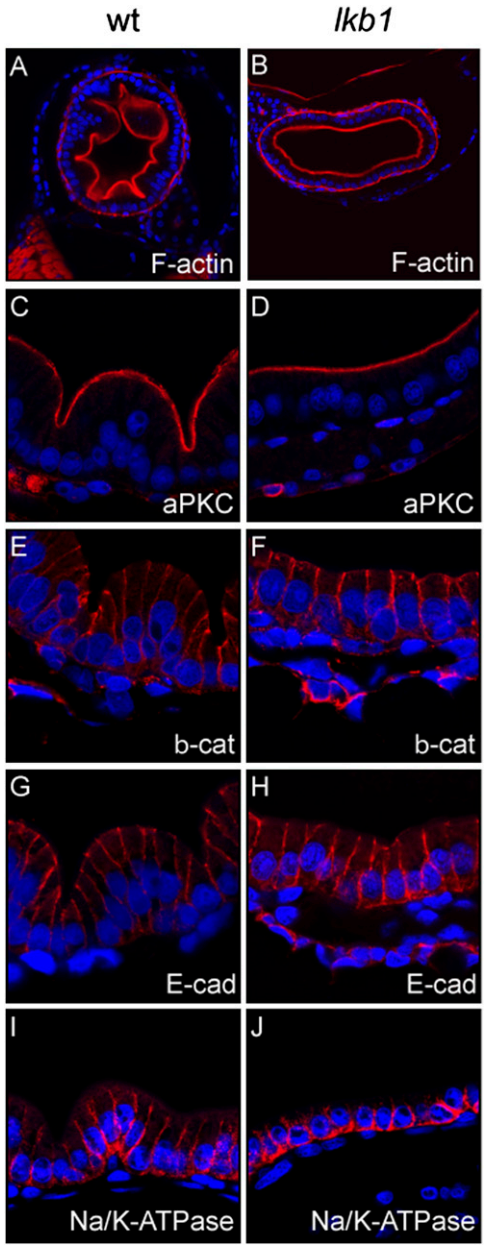

Fig. S2. There were no polarity defects in the intestine of *lkb1*-mutant larvae. Immunofluorescent analysis of transverse sections of the intestinal bulb in WT larvae (*A*, *C*, *E*, *G*, *I*, *K*) and *lkb1*-mutant larvae (*B*, *D*, *F*, *H*, *J*, *L*) at 7 dpf. Apical localization and levels of F-actin (*A* and *B*) and atypical PKC (aPKC) (*C* and *D*) are normal in *lkb1*-mutant larvae. Basolateral localization of β-catenin (*E* and *F*), E-cadherin (*G* and *H*), and Na/K ATPase (*I* and *J*), is not affected in *lkb1*-mutant larvae.

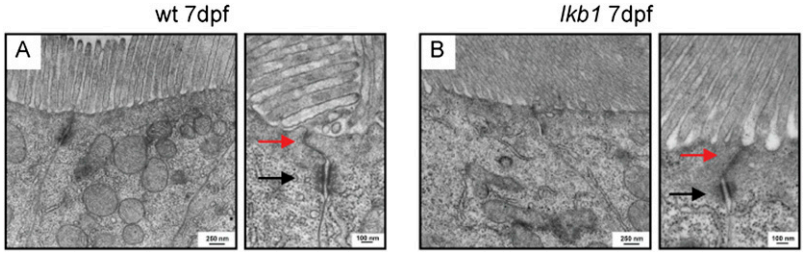

Fig. S3. Intact apical brush border and tight junctions in *lkb1*-mutant intestines. Transmission electron microscope micrographs of WT and *lkb1*-mutant intestinal cells at 7 dpf. (*A*) The microvilli constituting the apical brush border are depicted in the intestinal cells. (*B*) *Lkb1*-mutant intestinal cells also have microvilli and an apical brush border in their apical surface. Magnifications show hemidesmosomes (black arrows) and tight junctions (red arrows) in WT and *lkb1*-mutant intestinal cells.

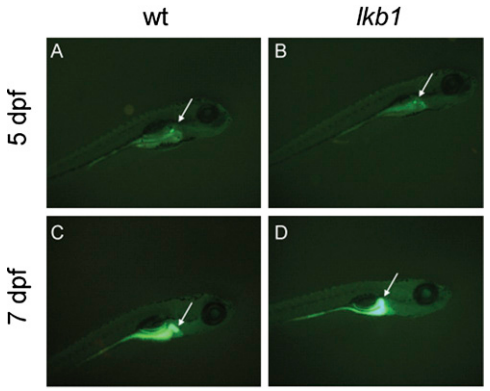

Fig. S4. Intestinal lipid processing is intact in *lkb1*-mutant larvae. Fluorescent live images of WT larvae (*A* and *C*) and *lkb1*-mutant larvae (*B* and *D*) incubated with 0.3 g/mL *N*-{[6-(2,4-dinitrophenyl)amino]hexanoyl}-1-palmitoyl-2-BODIPY-FL-pentanoyl-*sn*-glycero-3-phosphoethanolamine (PED6) for 2 h. Lateral views, anterior to the right. Cleavage of PED6 by phospholipase A2 (PLA2) relieves intramolar quenching and results in increased fluorescence. Gall bladder fluorescence (arrow in all panels) is observed because of rapid transport through the intestine and hepatobilary systems. In *lkb1*-mutant larvae, fluorescence in both the intestinal lumen and gall bladder was detected at levels equivalent to those in WT larvae.

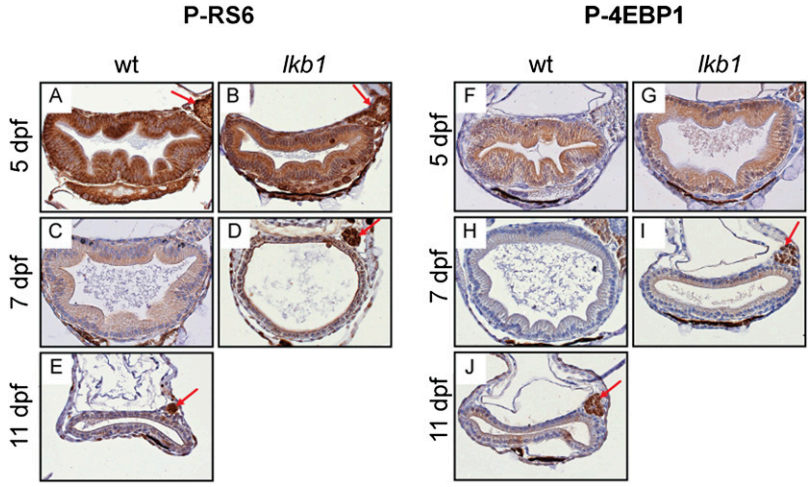

Fig. S5. Zebrafish TOR (zTOR) signaling is not grossly deregulated in *lkb1*-mutant intestine. Transverse sections of WT and *lkb1*-mutant intestines at indicated days of development were stained with an antibody against phospho-S6 ribosomal protein (RS6, Ser240/244) (*A*–*E*) and phospho-4EBP1 (Thr-37/46) (*F*–*J*). Strong phospho-RS6 staining is detected in WT and *lkb1*-mutant intestines at 5 dpf (*A* and *B*). Food-deprived WT larvae show moderate staining at 7 and 11 dpf (*C* and *E*). Staining in *lkb1* mutants (*B* and *D*) is not overtly different from staining in age-matched WT larvae (*A* and *C*). Moderate phospho-4EBP1 stating is detected in WT and *lkb1*-mutant intestines at 5 dpf. (*F* and *G*). Food-deprived WT larvae show decreased staining at 7 and 11 dpf (*H* and *J*). Staining in *lkb1* mutants is similar to that in age-matched WT larvae (*G* and *I*). Red arrows indicate expression in the pancreas.

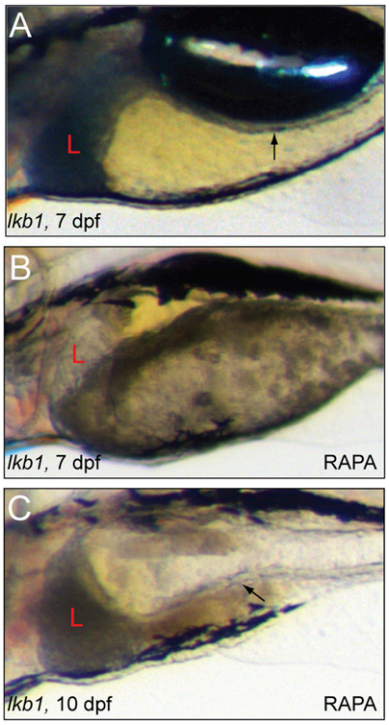

Fig. S6. Rapamycin treatment prolongs survival but is not sufficient to rescue the *lkb1* phenotype. (*A*) Untreated *lkb1*-mutant larva at 7 dpf. Note the black liver (L) and flat intestine (arrow). (*B*) Rapamycin-treated *lkb1*-mutant larva at 7 dpf shows a clear liver and some folding of the intestine. (*C*) Rapamycin-treated *lkb*-mutant larva at 10 dpf. Note the dark liver and flat intestine (arrow).

Fig. S7. Starvation induces intestinal *igfbp1* expression. Whole-mount RNA in situ hybridization with a probe against *igfbp1*. Lateral views, anterior to the left. (*A*) WT larvae at 7 dpf. *Igfbp1* is expressed in the liver. (*B*) *Lkb1*-mutant larva 7 dpf. *Igfbp1* is expressed in the liver and intestine. (*C*) Starved WT larvae at 11 dpf show a staining pattern similar to that in 7-dpf *lkb1*-mutant larvae.

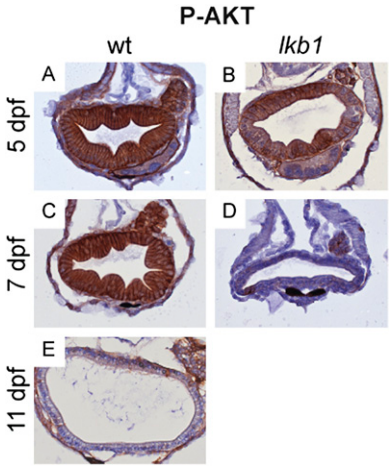

Fig. S8. Deregulation of PI3K signaling in *lkb1* mutants. Transverse sections of WT and *lkb1* intestines at indicated days of development were stained with an antibody against phosphorylated AKT. (*A* and *B*) Strong phospho-AKT staining is detected in WT and *lkb1*-mutant intestines at 5 dpf. WT intestine at 7 dpf is strongly stained (*C*), whereas in *lkb1*-mutant intestine at 7 dpf phospho-AKT staining is barely detectable (*D*). (*E*) Starved WT larvae at 11 dpf show very little phospho-AKT staining in the intestine.

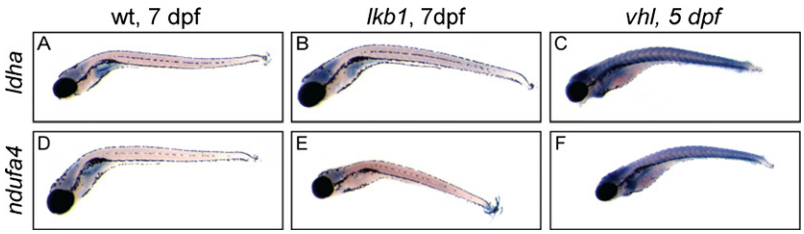

Fig. S9. The *lkb1*-mutant larvae are not hypoxic. Whole-mount in situ hybridization for expression of the hypoxia-inducible factor 1 subunit alpha (HIF1α) target genes *ldha* and *ndufa4* in WT (*A* and *D*), *lkb1*-mutant (*B* and *E*) and von Hippel–Lindau (*vhl*)-mutant (*C* and *F*) embryos. Lateral views, anterior to the left. (*A*) WT embryo at 7 dpf stained for *ldha1*; expression is detected in the brain. The same pattern is observed in *lkb1* embryos at 7 dpf (*B*), whereas *vhl*-mutant embryos that exhibit constitutive activation of the hypoxia program show up-regulation of *ldha1* expression throughout the embryo (*C*). (*D*) WT embryo at 7 dpf showing expression of *ndufa4* in the brain. The same pattern is observed in *lkb1*-mutant embryos at 7 dpf, whereas *vhl*-mutant embryos show widespread up-regulation of *ndufa4* expression.